Multiwall-Carbon-Nanotube-Reinforced Poly(ethylene terephthalate) Nanocomposites by Melt Compounding

Jun Young Kim,* Hawe Soo Park, Seong Hun Kim

Department of Fiber and Polymer Engineering, Center for Advanced Functional Polymers, Hanyang University, Seoul, 133-791, Korea

Received 30 August 2005; accepted 20 July 2006
DOI 10.1002/app.25377
Published online in Wiley InterScience (www.interscience.wiley.com).

ABSTRACT: Poly(ethylene terephthalate) (PET) nanocomposites reinforced with multiwall carbon nanotubes (MWCNTs) were prepared through melt compounding in a twin-screw extruder. The presence of MWCNTs, which acted as good nucleating agents, enhanced the crystallization of PET through heterogeneous nucleation. The incorporation of a small quantity of MWCNTs improved the thermal stability of the PET/MWCNT nanocomposites. The mechanical properties of the PET/MWCNT nanocomposites increased with even a small quantity of MWCNTs. There was a significant dependence of the rheological properties of the PET/MWCNT nanocomposites on the MWCNT content. The MWCNT loading increased the shear-thinning nature of the polymer-nanocomposite melt. The storage modulus and loss modulus of the PET/MWCNT nanocomposites increased with increasing frequency, and this increment effect was more pronounced at lower frequencies. At higher MWCNT contents, the dominant nanotube–nanotube interactions led to the formation of interconnected or networklike structures of MWCNTs in the PET/MWCNT nanocomposites. © 2006 Wiley Periodicals, Inc. J Appl Polym Sci 103: 1450–1457, 2007

Key words: compounding; nanocomposites; polyesters; reinforcement

INTRODUCTION

During the rapid advances in material science and technology, extensive research has been conducted on novel materials for various industrial applications. A great number of attempts have been made to develop high-performance polymer nanocomposites, using the benefits of nanotechnology, including the incorporation of nanoreinforcements into polymer matrices. Carbon nanotubes (CNTs) have attracted considerable attention as novel nanoreinforcements for advanced polymer nanocomposites in fields ranging from the scientific to the industrial since Iijima[1] first discovered them in 1991. In general, CNTs consist of a concentric cylinder of a single graphite layer or several graphite layers with diameters of 1–100 nm and lengths of 0.1–10 μm.[2] Fundamental research on CNTs has shown that the elastic modulus of CNTs can exceed 1.0 TPa, with tensile strengths in the range of 10–50 GPa,[3] suggesting potential applications as promising nanoreinforcements in advanced polymer nanocomposites because they exhibit remarkable physical characteristics such as high aspect ratios, large surface areas, and excellent mechanical properties.[4]

From an industrial perspective, the major challenges for high-performance polymer nanocomposites are to fabricate polymer nanocomposites with low costs and to facilitate large scale-up for commercial applications. Currently, three processing techniques are in common use for fabricating polymer nanocomposites: solution mixing, *in situ* polymerization, and melt compounding.[5,6] Among these processing techniques, melt compounding has been accepted as a simpler and more effective method than the other processing techniques, particularly from an industrial perspective, because this method makes it possible to fabricate high-performance polymer nanocomposites at low cost and to facilitate large scale-up for commercial applications. Furthermore, the combination of cheap thermoplastic polymers with a very small quantity of expensive CNTs is of great interest, in that this may provide attractive possibilities for improving the mechanical properties of polymer nanocomposites with low manufacturing costs.

However, because of their high cost and limited availability, only a few practical applications for CNT-based polymer nanocomposites in industrial fields have been realized to date. In addition, although several studies on CNT-filled polymer nanocomposites have been performed, their potential applications as nanoreinforcements have not been fully realized.[7] In this study, poly(ethylene terephthalate) (PET) nanocomposites reinforced with multiwall carbon nanotubes (MWCNTs) were prepared through melt compounding to fabricate high-performance polymer

**Present address:* Energy Corporate R&D Center, Samsung SDI Company, Limited, Korea.
Correspondence to: S. H. Kim (kimsh@hanyang.ac.kr).
Contract grant sponsor: Hanyang University; contract grant number: HY-2005-I.

nanocomposites at a low cost. The effects of the MWCNTs on the thermal, mechanical, and rheological properties of the PET/MWCNT nanocomposites are presented.

EXPERIMENTAL

Materials and preparation

The thermoplastic polymer was PET with an intrinsic viscosity of 1.07 dL/g; it was supplied by Hyo Sung Co. (Anyang, Korea). The nanotubes used as nanoreinforcements were MWCNTs (purity > 95%) synthesized through a thermal, chemical, vapor deposition process and purchased from Iljin Nanotechnology Co. (Seoul, Korea). All materials were dried at 120°C *in vacuo* for at least 24 h before use to minimize the effect of moisture. The PET/MWCNT nanocomposites were prepared through melt compounding with a Haake rheometer (Haake Technik GmbH, Vreden, Germany) equipped with a twin screw. The temperatures of the heating zone, from the hopper to the die, were set to 275, 285, 290, and 280°C, and the screw speed was fixed at 20 rpm. For the fabrication of the PET/MWCNT nanocomposites, the MWCNT contents were specified as 0.5, 1.0, and 2.0 wt % in the PET matrix.

Characterization

The morphology of the PET/MWCNT nanocomposites was observed with a JEOL JSM-6300F scanning electron microscope (Tokyo, Japan) and a JEOL 2000FX transmission electron microscope. The thermal behavior of the PET/MWCNT nanocomposites was measured with a TA Instrument 2010 differential scanning calorimeter (New Castle, DE) over the temperature range of 30–295°C at a scanning rate of 10°C/min under nitrogen. The thermogravimetric analysis (TGA) of the PET/MWCNT nanocomposites was performed with a TA Instrument SDF-2960 thermogravimetric analyzer under nitrogen over the temperature range of 30–900°C at a heating rate of 10°C/min. The mechanical properties of the PET/MWCNT nanocomposites were measured at room temperature with an Instron 4465 testing machine (Norwood, MA) according to the procedures in the ASTM D 638 standard. The gauge length and crosshead speed were set to 20 mm and 10 mm/min, respectively. The values of the mechanical properties in this study represented an average of the results for tensile tests of at least five samples. The rheological properties of the PET/MWCNT nanocomposites were measured at 270, 280, and 290°C, which covered the temperature processing window of polymer nanocomposites, with an ARES rheometer (Rheometric Scientific, Inc., Epsom, Surrey, UK). The dynamic shear measurements were performed in the oscillation mode and with parallel-plate geometry with a plate diameter of 25 mm and a plate-gap setting of approximately 1 mm. The frequencies were varied between 0.1 and 450 rad/s, and the strain amplitude was applied to be within the linear viscoelastic range.

RESULTS AND DISCUSSION

Scanning electron microscopy (SEM) and transmission electron microscopy (TEM) microphotographs of the pristine MWCNTs used in this study are shown in Figure 1. Nanotubes with hollow tubes in the center

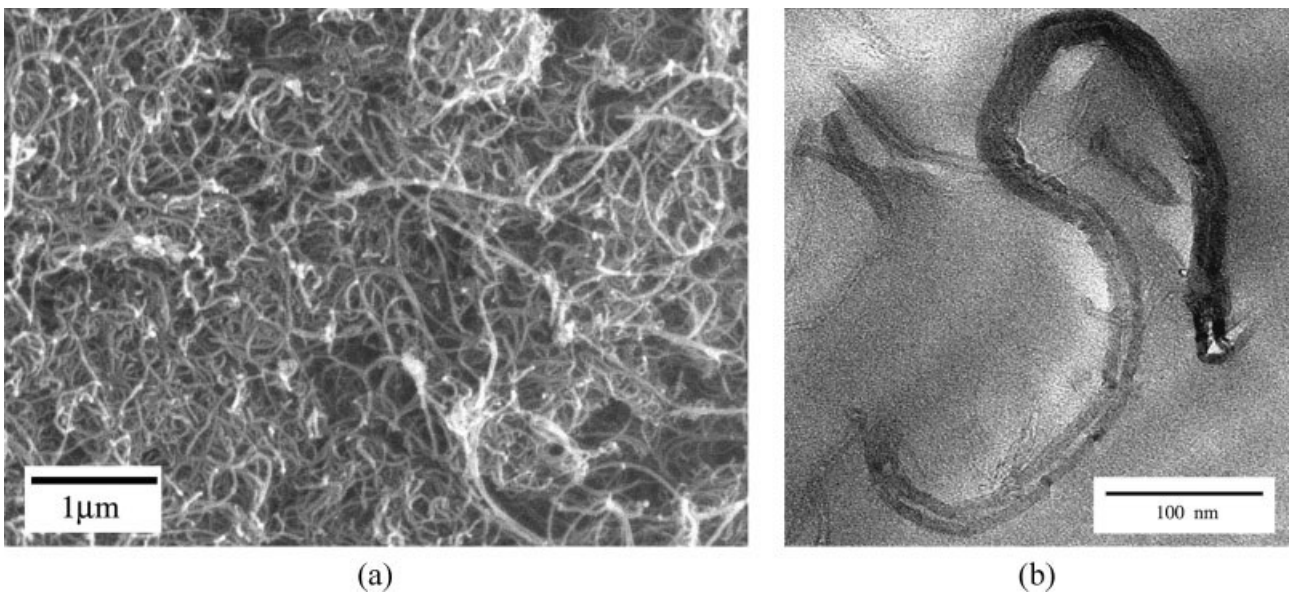

Figure 1 (a) SEM and (b) TEM images of pristine MWCNT.

TABLE I
DSC Results for the PET/MWCNT Nanocomposites with Respect to the MWCNT Content

Material	T_g (°C)[a]	T_m (°C)[a]	T_c (°C)[b]	ΔH_c (J/g)[b]	ΔT (°C)
PET	84.4	255.4	193.7	37.1	61.7
PET/MWCNT 0.5	84.0	255.3	213.9	40.3	41.4
PET/MWCNT 1.0	85.0	255.6	214.9	40.8	40.5
PET/MWCNT 2.0	84.9	254.2	216.6	41.7	37.6

[a] Obtained from DSC heating traces at a heating rate of 10°C/min.
[b] Obtained from DSC cooling traces at a cooling rate of 10°C/min.
ΔH_c is heat of crystallization.

are typical features observed in multiwall nanotubes that consist of several layers of coaxial CNTs. The MWCNTs have a diameter of approximately 10–40 nm and a length of several micrometers; this indicates that their aspect ratio reaches higher than 1000. In addition, the MWCNTs exhibit highly curved and random coiled features, which can be attributed to intrinsic van der Waals attractions between the individual nanotubes.[8]

Results from differential scanning calorimetry (DSC) thermograms of the PET/MWCNT nanocomposites are shown in Table I. The incorporation of MWCNTs into the PET matrix had little effect on the glass-transition temperature (T_g) and melting temperature (T_m) of the PET/MWCNT nanocomposites. As the MWCNT content increased, the crystallization temperature (T_c) of the PET/MWCNT nanocomposites increased, this effect being more significant at lower MWCNT contents. MWCNTs promoted the formation of heterogeneous nuclei, with lower energy consumption required to reach critical stability for crystal growth,[9] resulting in an effective function as nucleating agents in the PET/MWCNT nanocomposites. As shown in Table I, the increase in T_c of the PET/MWCNT nanocomposites with increasing MWCNT content, together with the fact that the degree of supercooling ($\Delta T = T_m - T_c$) for crystallization decreased with increasing MWCNT content, suggested that MWCNTs could effectively act as nucleating agents in the PET/MWCNT nanocomposites. Therefore, the incorporation of a very small quantity of MWCNTs could effectively enhance the crystallization of the PET matrix through heterogeneous nucleation.

TABLE II
Thermal Stability of the PET/MWCNT Nanocomposites as a Function of the MWCNT Content

Material	IDT (°C)	T_{max} (°C)	T_{60} (°C)[a]	IPDT (°C)	W_R (%)[b]
PET	382.3	431.9	439.7	471.9	5.7
PET/MWCNT 0.5	383.5	432.8	441.1	492.6	9.4
PET/MWCNT 1.0	385.2	433.1	441.9	500.3	12.6
PET/MWCNT 2.0	386.4	437.6	446.2	518.4	16.7

[a] Decomposition temperature at a 60% weight loss.
[b] Residual yield in TGA curves at 800°C.

Results from TGA thermograms of the PET/MWCNT nanocomposites as a function of the MWCNT content are shown in Table II. The thermal stability factors, such as the initial thermal decomposition temperature (IDT), thermal decomposition temperature at the maximum rate (T_{max}), and integral procedure decomposition temperature (IPDT), are in common use to estimate the thermal stability of a polymeric material.[10] As the MWCNT content increased, the values of IDT, T_{max}, and IPDT as well as the residual yield of the PET/MWCNT nanocomposites increased, and this indicated the enhancement of the thermal stability of the polymer nanocomposites by the incorporation of MWCNTs. The improvement in the thermal stability of the PET/MWCNT nanocomposites could be attributed to a physical barrier effect with the incorporation of MWCNTs that prevented the diffusion of volatile, decomposed products out of the polymer nanocomposites, leading to the retardation of the thermal decomposition in the PET/MWCNT nanocomposites. Kashiwagi and coworkers[11] reported that CNT layers exhibited a good barrier effect on the thermal degradation process, and they could not only insulate polymers but also reduce the weight-loss rate of thermal degradation products, resulting in a significant improvement in the thermal stability of the polymer nanocomposites. Thus, it could be deduced that a small quantity of MWCNTs was beneficial, in that they acted as effective thermal-decomposition-resistant nanoreinforcements in the PET matrix, improving the thermal stability of the PET/MWCNT nanocomposites.

The variations of the tensile strength and tensile modulus of the PET/MWCNT nanocomposites with the MWCNT content are shown in Figure 2. There was a significant dependence of the mechanical properties

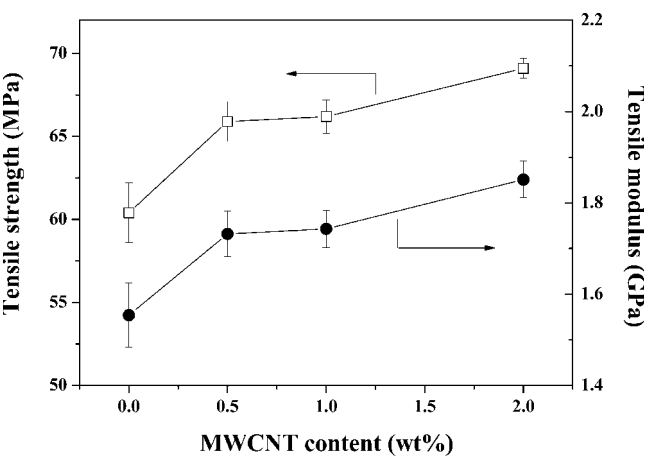

Figure 2 Effect of MWCNTs on the tensile strength and tensile modulus of PET/MWCNT nanocomposites.

of the PET/MWCNT nanocomposites on the MWCNT content. The incorporation of MWCNTs increased the tensile strength and tensile modulus of the PET/MWCNT nanocomposites, this improvement being more significant with lower MWCNT contents. Gorga and coworkers[12] reported an improvement in the mechanical properties via nanotube orientation by melt drawing after melt compounding in a poly(methyl methacrylate) matrix with low levels ($\sim$ 1 wt %) of MWCNTs. The enhancement of the tensile strength and modulus of the PET/MWCNT nanocomposites could be attributed to the reinforcement effect of MWCNTs with a high aspect ratio and their uniform dispersion in the PET matrix. However, this improvement in the mechanical properties of the PET/MWCNT nanocomposites was not increased at higher MWCNT contents, as expected, in comparison with that at lower contents. This result may also be related to the fact that CNTs have a tendency to bundle together and to form some agglomeration because of intrinsic van der Waals attractions between the individual nanotubes, preventing efficient load transfer to the polymer matrix.[2,8] SEM images of the fracture surfaces for the PET/MWCNT nanocomposites are shown in Figure 3. Some MWCNT bundles were pulled out from the PET matrix, and this indicated that some of the nanotube bundles were individually dispersed in the polymer matrix. At lower MWCNT contents, the PET/MWCNT nanocomposites exhibited a relatively uniform dispersion of the MWCNTs in the PET matrix, in comparison with the nanocomposites with higher MWCNT contents. As shown in Figure 3(b), less uniformly dispersed and highly entangled MWCNTs could be observed in the polymer nanocomposites with higher MWCNT contents. In addition, MWCNTs were randomly oriented and formed interconnecting structures in the polymer nanocomposites. Nanotubes with a small size, high aspect ratio, and large surface area are often subjected to self-agglomeration or bundle formation at higher concentrations and thus easily form interconnected or networklike structures in the molten polymer matrix.[2,7,8]

A comparative study of the experimental results for the PET/MWCNT nanocomposites with the values calculated from theoretical models is shown in Figure 4. By assuming that the PET/MWCNT nanocomposites are randomly oriented, discontinuous fiber laminae, we can calculate the composite modulus (E_C) with the modified Halpin–Tsai equation[13,14]:

$$E_C = \left[\left(\frac{3}{8}\right)\left(\frac{1 + 2(l_{\mathrm{MWCNT}}/d_{\mathrm{MWCNT}})\eta_L V_{\mathrm{MWCNT}}}{1 - \eta_L V_{\mathrm{MWCNT}}}\right) + \left(\frac{5}{8}\right)\left(\frac{1 + 2\eta_T V_{\mathrm{MWCNT}}}{1 - \eta_T V_{\mathrm{MWCNT}}}\right)\right] E_{\mathrm{PET}} \quad (1)$$

where

$$\eta_L = \frac{(E_{\mathrm{MWCNT}}/E_{\mathrm{PET}}) - 1}{(E_{\mathrm{MWCNT}}/E_{\mathrm{PET}}) + 2(l_{\mathrm{MWCNT}}/d_{\mathrm{MWCNT}})}$$

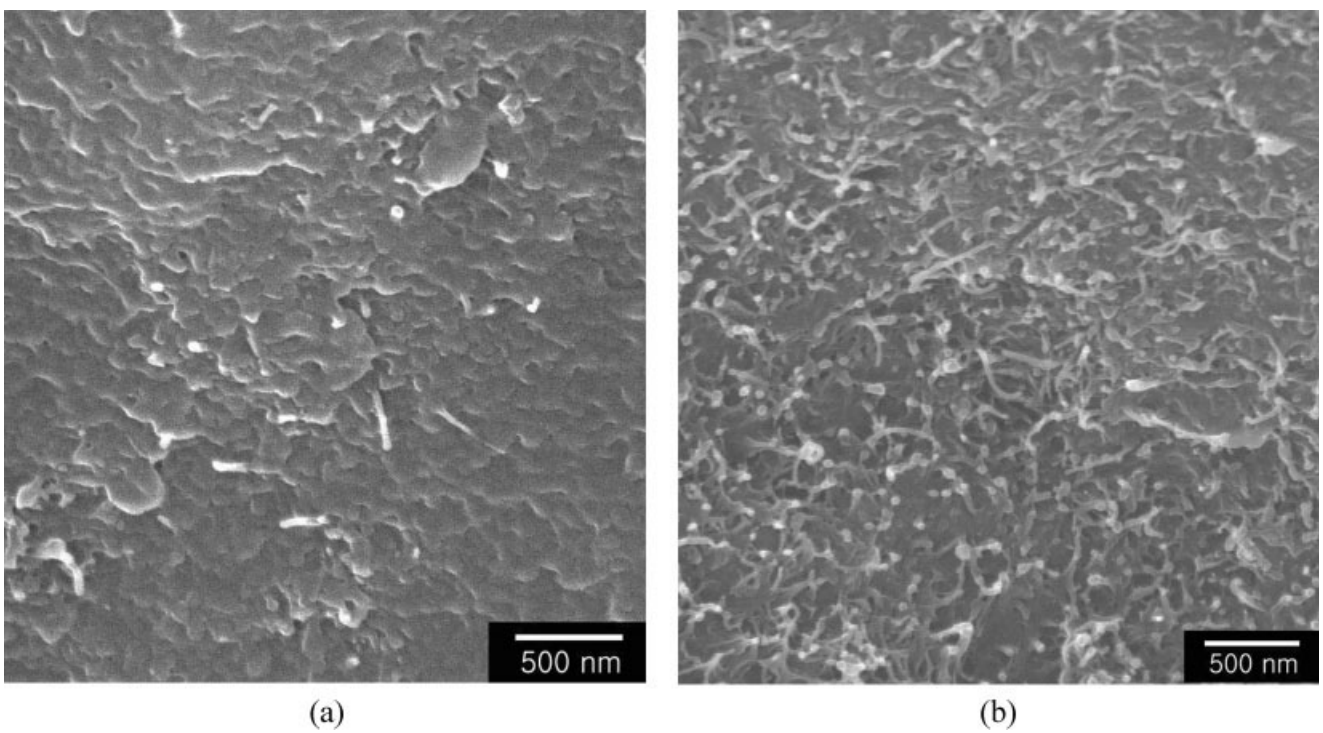

Figure 3 SEM images of the fracture surfaces of PET/MWCNT nanocomposites containing (a) 0.5 and (b) 2.0 wt % MWCNT.

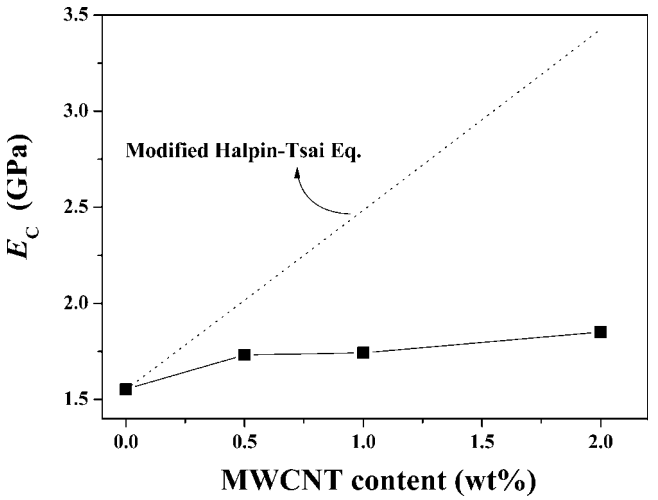

Figure 4 Experimental composite modulus (E_C) of PET/MWCNT nanocomposites and theoretical values calculated from eq. (1) as a function of the MWCNT content.

and

$$\eta_T = \frac{(E_{\mathrm{MWCNT}}/E_{\mathrm{PET}}) - 1}{(E_{\mathrm{MWCNT}}/E_{\mathrm{PET}}) + 2}$$

E_{PET} and E_{MWCNT} represent the moduli of PET and MWCNT, $l_{\mathrm{MWCNT}}/d_{\mathrm{MWCNT}}$ is the ratio of the length to the diameter for the nanotubes, and V_{MWCNT} is the volume faction of the nanotubes in the nanocomposites. To fit eq. (1) to the experimental results for the PET/MWCNT nanocomposites, the weight fraction was transformed to the volume faction with the densities of PET (1.34 g/cm^3) and perfectly graphitized MWCNTs (2.16 g/cm^3).[14] The theoretical values of the composite modulus were estimated under the assumption of an aspect ratio of $\sim$ 1000 and an MWCNT modulus of $\sim$ 450 GPa for the nanotubes. The MWCNT modulus used in this study represents a midrange value in the modulus ranges of nanotubes previously measured.[14] As shown in Figure 4, the composite moduli of the PET/MWCNT nanocomposites were much lower than the theoretical values calculated with eq. (1), and the deviation from the theoretical values was larger with increasing MWCNT content. For single-wall nanotubes (SWNTs) and polypropylene (PP) composite fibers, Sokolov et al.[15] reported that the experimental value of the composite modulus at a 1 wt % SWNT concentration was in good agreement with the theoretical calculation, whereas the negative deviation was greater with an increasing SWNT concentration up to 5 wt %, and they suggested that the large negative deviation could be attributed to the poor distribution of SWNTs, which became even more heterogeneous in the PP matrix with increasing SWNT concentration. Gorga and coworkers[12] reported that adding a low level of MWCNTs to PP improved the mechanical properties up to an optimal concentration (0.25 wt %), above which nanotube aggregation led to a property decrease via stress concentration. Furthermore, according to the rule of mixtures, the maximum modulus of the PP/MWCNT composites should reach 2.2 GPa at a loading of 0.25 wt % MWCNTs. However, because of a less than optimal load transfer, the maximum modulus was 1.3 GPa at a loading of 0.25 wt % MWCNTs. They suggested that poor adhesion to the matrix material and imperfections and defects in the nanotube structure would also result in a reduced composite modulus.[12] For achieving a further enhancement of the mechanical properties of polymer nanocomposites, our current research is aimed at improving the dispersion of MWCNTs and the interfacial adhesion between the polymer matrix and MWCNTs through chemical functionalization of the nanotubes.

Variations of the complex viscosity ($|\eta^*|$) of the PET/MWCNT nanocomposites with the MWCNT content at 270°C as a function of the frequency are shown in Figure 5(a). $|\eta^*|$ of the PET/MWCNT nanocomposites decreased with increasing frequency, and this indicated non-Newtonian behavior. The shear-thinning behavior observed in the PET/MWCNT nanocomposites could be attributed to the orientation of rigid molecular chains in the polymer nanocomposites during the applied shear force. The effect of MWCNTs on $|\eta^*|$ of the PET/MWCNT nanocomposites was more pronounced at a low frequency than at a high frequency, and this effect was reduced with increasing frequency because of the strong shear-thinning behavior of the polymer nanocomposites with the addition of MWCNTs. In addition, $|\eta^*|$ of the PET/MWCNT nanocomposites increased with increasing MWCNT content, and this could be attributed to the physical interactions between the polymer and nanotubes and between the nanotubes and nanotubes. This increment effect was closely related to the large increase in the storage modulus (G'), which is described in the following section. As shown in Figure 5(b), $|\eta^*|$ of the PET/MWCNT 2.0 nanocomposite decreased with increasing temperature. In a low-frequency region, the temperature had little effect on $|\eta^*|$ of the PET/MWCNT nanocomposites. However, in a high-frequency region, the rheological properties of PET/MWCNT were affected by the temperature, and $|\eta^*|$ significantly decreased with increasing temperature.

The variations of G' and the loss modulus (G'') of MWCNT-reinforced PET nanocomposites at 270°C are shown in Figure 6. G' and G'' of the PET/MWCNT nanocomposites were higher than those of pure PET and increased with increasing MWCNT content. In addition, G' and G'' of the PET/MWCNT nanocomposites increased with increasing frequency, this increment being more significant at a low frequency than

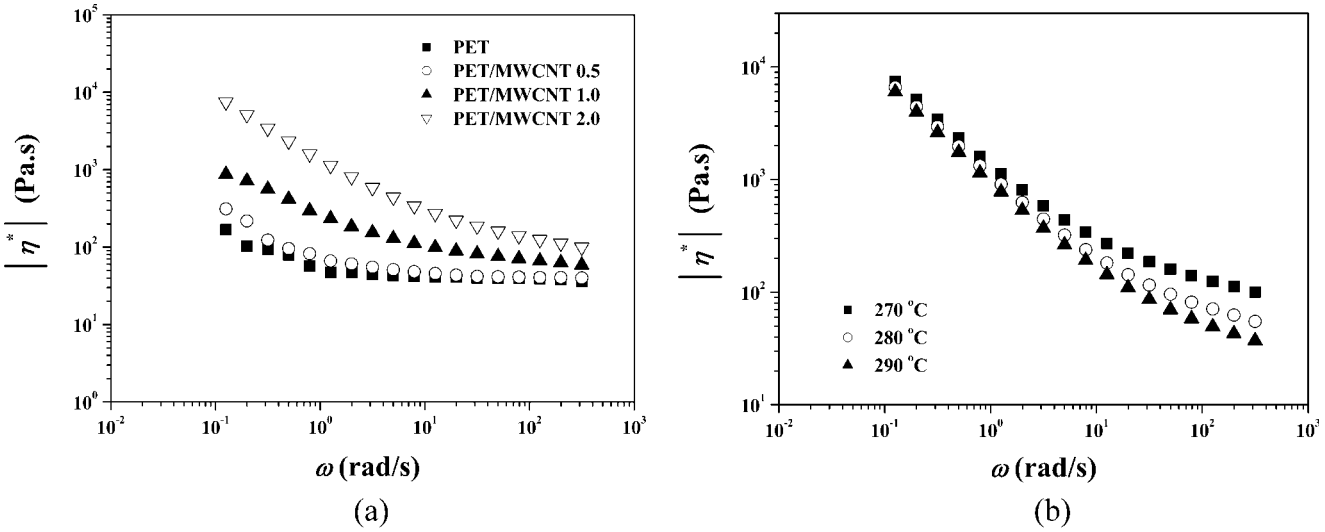

Figure 5 |η*| of (a) PET/MWCNT nanocomposites with different MWCNT contents at 270°C and (b) PET/MWCNT 2.0 nanocomposites at different temperatures as a function of the frequency (ω).

at a high frequency. This phenomenon was similar to the tendency observed in the variations of |η*| of the PET/MWCNT nanocomposites with increasing MWCNT content. As the MWCNT content increased, the physical interactions between the nanotubes could lead to the formation of interconnected or networklike structures of the nanotubes in the polymer matrix.[16] The extent of the increase in G' of the PET/MWCNT nanocomposites was higher than that of G'' over the frequency range studied, this effect being more pronounced in a lower frequency region. These rheological responses are similar to the relaxation behavior of typical filled-polymer composite systems.[17] To understand the effect of MWCNTs on the rheological behavior of the PET/MWCNT nanocomposites, it is instructive to characterize the variations of the slopes of the plots of |η*| and G' versus the frequency for the PET/MWCNT nanocomposites. The nonterminal behavior observed in a low-frequency region in the PET/MWCNT nanocomposites may be related to the variation of the terminal slope of the flow curves, such as the shear-thinning exponent in the plot of |η*| versus the frequency and the relaxation exponent in the plot of G' versus the frequency.[18] In the case of an ideal Newtonian fluid, the shear-thinning exponent approaches or equals zero, and the viscosity is independent of the frequency, thereby exhibiting terminal flow behavior, whereas in nanocomposites, as the shear-thinning behavior develops, the shear-thinning exponent increases with increasing filler

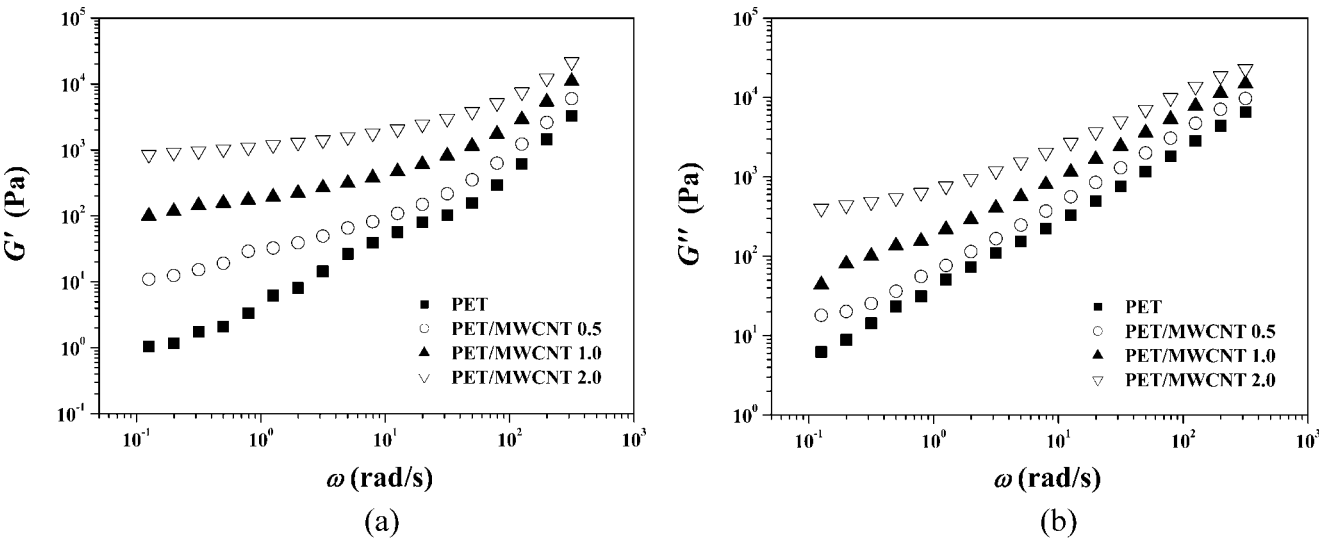

Figure 6 Effect of MWCNTs on (a) G' and (b) G'' of PET/MWCNT nanocomposites at 270°C as a function of the frequency (ω).

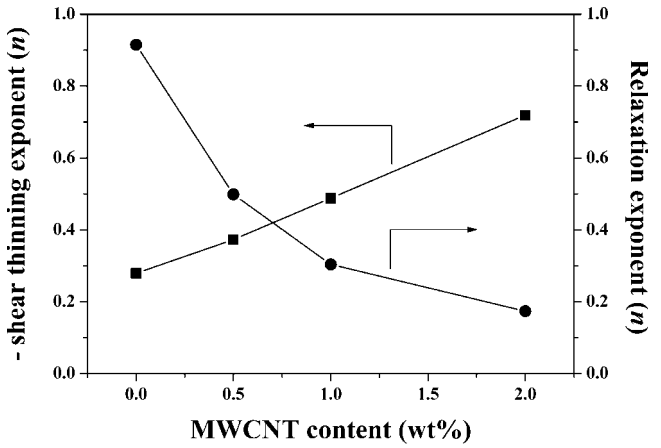

Figure 7 Variation of the shear-thinning exponent and relaxation exponent of the PET/MWCNT nanocomposites with the MWCNT content.

loading.[18] The shear-thinning exponent and relaxation exponent of the PET/MWCNT nanocomposites obtained by the fitting of the experimental data in a low-frequency region to power-law equations, such as $|\eta^*| \approx \omega^n$ (where ω is the frequency and n is the shear-thinning exponent) and $G' \approx \omega^n$ (where ω is the frequency and n is the relaxation exponent),[18] are shown in Figure 7. The shear-thinning exponent of the PET/MWCNT nanocomposites decreased with increasing MWCNT content, indicating the significant dependence of the shear-thinning behavior of the polymer nanocomposites on the MWCNT content. In addition, the relaxation exponent of the PET/MWCNT nanocomposite decreased with increasing MWCNT content. This result can be explained by the fact that the nanotube–nanotube interactions were more dominant with increasing MWCNT content, leading to the formation of interconnected structures of the nanotubes in the polymer nanocomposites. The tendency to form interconnected structures between the nanotubes in these PET/MWCNT nanocomposite systems was increased by the dominant nanotube–nanotube interactions at higher contents, and the result of these effects was the transition of the polymer-nanocomposite melt from a liquidlike state to a pseudo-solidlike state, which was reflected in the changes in the values of the shear-thinning exponent and relaxation exponent.[18] Plots of the phase angle versus the absolute value of the complex modulus ($|G^*|$), which are known as van Gurp–Palmen plots,[19] for the PET/MWCNT nanocomposites at 270°C are shown in Figure 8. A significant change in the phase angle occurred with the addition of MWCNTs. A decrease in the phase angle with decreasing $|G^*|$ indicated an increase in the elastic behavior. The PET/MWCNT nanocomposites exhibited smaller phase angles at lower $|G^*|$ values with increasing MWCNT content, and this implied that the incorporation of MWCNTs enhanced the elasticity of the PET/MWCNT nanocomposites.

As described in the previous section, G' and G'' of the PET/MWCNT nanocomposites were higher than those of PET and increased with increasing MWCNT content. Cole–Cole plots of the PET/MWCNT nanocomposites with the MWCNT content are shown in Figure 9. The PET/MWCNT nanocomposites had lower slopes with higher G' values at a low G'' value, and this indicated that the PET/MWCNT nanocomposite systems were heterogeneous with the nanotube–nanotube interactions. However, in a higher frequency region, the slopes of the Cole–Cole plots for the PET/MWCNT nanocomposites increased and approached a slope of approximately 2 or one similar to that of PET. These results indicated that some interconnected or networklike structures that formed in

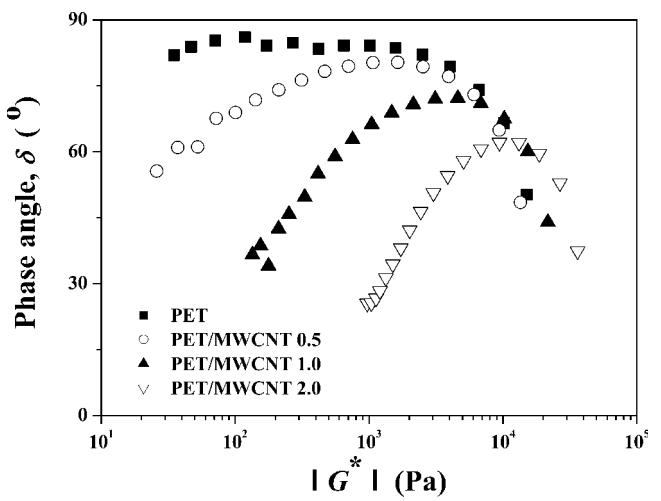

Figure 8 Plots of the phase angle versus $|G^*|$ for PET/MWCNT nanocomposites measured at 270°C.

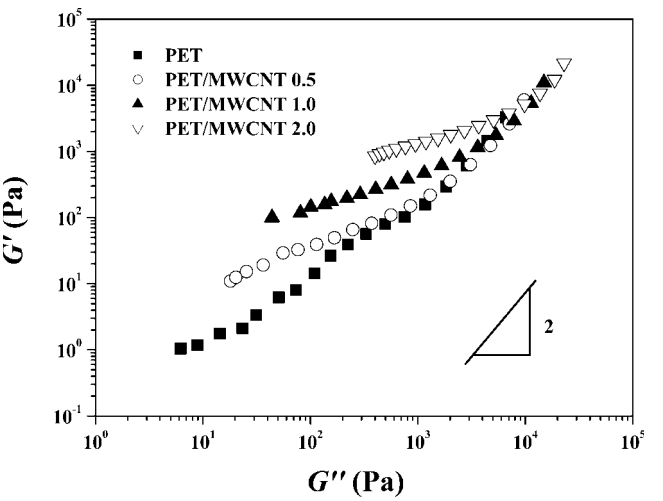

Figure 9 Cole–Cole plots of PET/MWCNT nanocomposites with the MWCNT content.

the polymer nanocomposites because of the nanotube–nanotube interactions may have been broken by a high shearing force, and the polymer nanocomposites became an isotropic and homogeneous system with the shear force.[20] In addition, the slopes of the plots of G' and G'' for the PET/MWCNT nanocomposites decreased with increasing MWCNT content, and this indicated that the addition of MWCNTs had a significant effect on the microstructures of the PET/MWCNT nanocomposites. Pötschke et al.[21] investigated the rheological behavior of CNT/polycarbonate composites prepared via melt blending in an extruder, and they suggested that the shift and change in the slope of the plots of G' versus G'' for CNT/polycarbonate composites indicated a significant change in the microstructures of the polymer composites with the addition of CNTs. For a detailed analysis, our research currently in progress is aimed at characterizing the microstructures of PET/MWCNT nanocomposites with small-angle X-ray measurements.

CONCLUSIONS

PET/MWCNT nanocomposites were prepared through melt compounding in a twin-screw extruder, and the effects of MWCNTs on the thermal, rheological, and mechanical properties of the PET/MWCNT nanocomposites were investigated. The presence of MWCNTs, which effectively acted as nucleating agents, enhanced the crystallization of PET through heterogeneous nucleation. The incorporation of a small quantity of MWCNTs improved the mechanical properties of the PET/MWCNT nanocomposites, and this was attributed to the reinforcement effect of MWCNTs with a high aspect ratio and their uniform dispersion in the PET matrix. There was a significant dependence of the rheological behavior of the PET/MWCNT nanocomposites on the MWCNT content. As the MWCNT content increased, the nanotube–nanotube interactions were more dominant, and some interconnected or networklike structures formed in the PET/MWCNT nanocomposites. The PET/MWCNT nanocomposites exhibited smaller phase angles at lower $|G^*|$ values with increasing MWCNT content, and this implied that the elastic behavior of the PET/MWCNT nanocomposites was enhanced by the incorporation of MWCNTs. The decrease in the slopes of the plots of G' and G'' for the PET/MWCNT nanocomposites with increasing MWCNT content suggested that the microstructures of the PET/MWCNT nanocomposites was affected by the addition of MWCNTs.

References

1. Iijima, S. Nature 1991, 354, 56.
2. (a) Iijima, S.; Ichihashi, T. Nature 1993, 363, 603; (b) Dresselhaus, M. S.; Dresselhaus, G.; Avouris, P. H. Carbon Nanotubes: Synthesis, Structure, Properties, and Applications; Springer: Berlin, 2001; (c) Laurent, C.; Peigney, A. In Encyclopedia of Nanoscience and Nanotechnology; Nalwa, H. S., Ed.; American Scientific: Stevenson Ranch, CA, 2004; Vol. 1, p 635.
3. (a) Goze, C.; Bernier, P.; Henrard, L.; Vaccarini, L.; Hernandez, E.; Rubio, A. Synth Met 1999, 103, 2500; (b) Wong, E. W.; Sheehan, P. E.; Lieber, C. M. Science 1997, 277, 1971; (c) Yao, Z.; Zhu, C. C.; Cheng, M.; Liu, J. Comput Mater Sci 2001, 22, 180; (d) Yu, M. F.; Files, B. S.; Arepalli, S.; Ruoff, R. S. Phys Rev Lett 2000, 84, 5552.
4. Antonucci, V.; Hsiao, K. T.; Advani, S. G. In Advanced Polymeric Materials: Structure Property Relationships; Shonaike, G. O.; Advani, S. G., Eds.; CRC: New York, 2003; Chapter 11, p 397.
5. (a) Haggenmuller, R.; Conmas, H. H.; Rinzler, A. G.; Fischer, J. E.; Winey, K. I. Chem Phys Lett 2000, 330, 219; (b) Jia, Z. J.; Wang, Z. Y.; Liang, J.; Wei, B. Q.; Wu, D. H. Mater Sci Eng A 1999, 271, 395; (c) Jin, Z.; Pramoda, K. P.; Goh, S. H.; Xu, G. Mater Res Bull 2002, 37, 271.
6. (a) Kim, J. Y.; Kim, S. H. J Polym Sci Part B: Polym Phys 2006, 44, 1062; (b) Kim, J Y.; Park, H. S.; Kim, S. H. Polymer 2006, 47, 1379; (c) Kim, J. Y.; Park, H. S.; Kim, S. H. Polym Degrad Stab, submitted; (d) Kim, J. Y.; Kim, S. H. Polym Eng Sci, submitted.
7. (a) Schadler, L. S.; Giannaris, S. C.; Ajayan, P. M. Appl Phys Lett 1998, 73, 3842; (b) Wong, M.; Paramsothy, M.; Xu, X. J.; Ren, Y.; Li, S.; Liao, K. Polymer 2003, 44, 7757; (c) Frankland, S. J. V.; Harik, V. M. Surf Sci 2003, 525, L103.
8. Ebbesen, T. Carbon Nanotubes: Preparation and Properties; CRC: New York, 1997.
9. Vincent, B. F. Calorimetry and Thermal Analysis of Polymers; Springer: Berlin, 2001.
10. Park, S. J.; Cho, M. S. J Mater Sci 2000, 35, 3525.
11. (a) Kashiwagi, T.; Grulke, E.; Hilding, J.; Harris, R.; Awad, W.; Douglas, J. Macromol Rapid Commun 2002, 23, 761; (b) Kashiwagi, T.; Shields, J. R.; Harris, R. H.; Davis, R. D. J Appl Polym Sci 2003, 87, 1541.
12. (a) Gorga, R. E.; Cohen, R. E. J Polym Sci Part B: Polym Phys 2004, 42, 2690; (b) Dondero, W. E.; Gorga, R. E. J Polym Sci Part B: Polym Phys 2006, 44, 864.
13. Mallick, P. K. Fiber-Reinforced Composites; Marcel Dekker: New York, 1993.
14. (a) Qian, D.; Dickey, E. C.; Andrews, R.; Rantall, T. Appl Phys Lett 2000, 76, 2868; (b) Wong, E. W.; Sheehan, P. E.; Lieber, C. M. Science 1997, 277, 1971.
15. Chang, T. E.; Jensen, L. R.; Kisliuk, A.; Pipes, R. B.; Pyrz, R.; Sokolov, A. P. Polymer 2005, 46, 439.
16. Seo, M. K.; Park, S. J. Chem Phys Lett 2004, 395, 44.
17. (a) Enikolopyan, N. S.; Fridman, M. L.; Stalnova, I. U.; Popov, V. L. Adv Polym Sci 1990, 96, 1; (b) Krishnamoorti, R.; Vaia, R. A.; Giannelis, E. P. Chem Mater 1996, 8, 1728.
18. (a) Costa, F. R.; Wagenknecht, U.; Jehnichen, D.; Abdel-Goad, M.; Heinrich, G. Polymer 2006, 47, 1649; (b) Abdel-Goad, M.; Pötschke, P. J Non-Newtonian Fluid Mech 2005, 128, 2; (c) Wagener, R.; Reisinger, T. J. G. Polymer 2003, 44, 7513.
19. (a) Van Gulp, M.; Palmen, J. Rheol Bull 1998, 67, 5; (b) Trinkle, S.; Friedrich, C. Rheol Acta 2002, 41, 103.
20. Han, C. D.; Kim, J.; Kim, J. K. Macromolecules 1989, 22, 383.
21. Pötschke, P.; Fornes, T. D.; Paul, D. R. Polymer 2002, 43, 3247.